Electronic Supplementary Material (ESI) for Physical Chemistry Chemical Physics.

Supporting Information

Exploring Mechanochemical Reactions at the Nanoscale: Theory Versus Experiment

Nicholas Hopper,[1] François Sidoroff,[2] Resham Rana,[1] Robert Bavisotto,[1] Juliette Cayer-Barrioz,[2] Denis Mazuyer [2] and Wilfred T Tysoe [1 *]

[1] *Department of Chemistry and Biochemistry, University of Wisconsin-Milwaukee, Milwaukee, WI 53211, USA*

[2] *Laboratoire de Tribologie et Dynamique des Systèmes, CNRS UMR5513, Ecole Centrale de Lyon, F-69134 Ecully cedex, France*

See video

Figure S1: Evolution of the structures of methyl thiolate on Cu(100) as it evolves from the reactant to the transition state to initiate C–S bond scission.

See video

Figure S2: Movies of the evolution in the initial (Left) and transition-state (Right) structures of methyl thiolate compressed by hydrogen-terminated Cu(100) slabs as they are brought closer together. The energy versus distance profiles are used to calculate the normal-stress dependent reaction rates.

1. Atomic Coordinates for the Compression of Methyl Thiolate Species on Cu(100)

VASP POSCAR file: Initial coordinates for compression – (8.5 Ångström slab separation)

```
Cu100+MeS
  1.00000000000000
    5.0553315674999997    0.0000000000000000    0.0000000000000000
    0.0000000000000000    5.0553315674999997    0.0000000000000000
    0.0000000000000000    0.0000000000000000   42.8959085157000004
  Cu   S   C   H
   36   1   1   11
Selective dynamics
Direct
  0.2500000000000000  0.2500000000000000  0.4064874299589221   F   F   F
  0.2500000000000000  0.7500000000000000  0.4064874299589221   F   F   F
  0.7500000000000000  0.2500000000000000  0.4064874299589221   F   F   F
  0.7500000000000000  0.7500000000000000  0.4064874299589221   F   F   F
```

0.0000000000000000 0.0000000000000000 0.4481540965606072 F F F
0.0000000000000000 0.5000000000000000 0.4481540965606072 F F F
0.5000000000000000 0.0000000000000000 0.4481540965606072 F F F
0.5000000000000000 0.5000000000000000 0.4481540965606072 F F F
0.2500000000000000 0.2500000000000000 0.4898207632602052 F F F
0.2500000000000000 0.7500000000000000 0.4898207632602052 F F F
0.7500000000000000 0.2500000000000000 0.4898207632602052 F F F
0.7500000000000000 0.7500000000000000 0.4898207632602052 F F F
0.0000000000000000 0.0000000000000000 0.0000000000000000 F F F
0.0000000000000000 0.5000000000000000 0.0000000000000000 F F F
0.5000000000000000 0.0000000000000000 0.0000000000000000 F F F
0.5000000000000000 0.5000000000000000 0.0000000000000000 F F F
0.2500000000000000 0.2500000000000000 0.0416666666995980 F F F
0.2500000000000000 0.7500000000000000 0.0416666666995980 F F F
0.7500000000000000 0.2500000000000000 0.0416666666995980 F F F
0.7500000000000000 0.7500000000000000 0.0416666666995980 F F F
0.0000000000000000 0.0000000000000000 0.0833333332989454 F F F
0.0000000000000000 0.5000000000000000 0.0833333332989454 F F F
0.5000000000000000 0.0000000000000000 0.0833333332989454 F F F
0.5000000000000000 0.5000000000000000 0.0833333332989454 F F F
0.2487478658982809 0.2484632622690128 0.1253649888228665 T T T
0.2487094855903393 0.7511623930340718 0.1253565617212047 T T T
0.7514118450436698 0.2484641045129408 0.1253596523441942 T T T
0.7514441193627448 0.7511587421728549 0.1253501141138500 T T T
0.0001862375417190 0.9997047204773111 0.1686181472557280 T T T
0.0002163623058209 0.4997443347865556 0.1675114729113147 T T T
0.5001921561379916 0.9996094776963957 0.1675118913712268 T T T
0.5001283246912891 0.4997762673735906 0.1663271182483825 T T T
0.2444418449959826 0.2436141023956822 0.2101933085981429 T T T
0.2443477124302262 0.7554838859020592 0.2102199192227800 T T T
0.7560154991360761 0.2439521024926066 0.2101608678466391 T T T
0.7560027762664703 0.7553141378744144 0.2101877241962384 T T T
0.4963605823430252 0.49621124380011633 0.2431877660260895 T T T
0.4933759913706979 0.4913106565734809 0.2860588659017509 T T T
0.5889234195995878 0.6720785335430404 0.2946273348415502 T T T
0.2873017915898882 0.4827152934901088 0.2940063076469315 T T T
0.6021412349130476 0.31619203727927186 0.294041839001288 T T T
0.0000000000000000 0.0000000000000000 0.3933212761584599 T T T
0.5000000000000000 0.0000000000000000 0.3933212761584599 T T T
0.0000000000000000 0.5000000000000000 0.3933212761584599 T T T
0.5000000000000000 0.5000000000000000 0.3933212761584599 T T T
0.0000000000000000 0.0000000000000000 0.5029869170606673 F F F
0.5000000000000000 0.0000000000000000 0.5029869170606673 F F F
0.0000000000000000 0.5000000000000000 0.5029869170606673 F F F
0.5000000000000000 0.5000000000000000 0.5029869170606673 F F F

2. Background Subtraction in the Calculations of the Energy versus Slab Separation

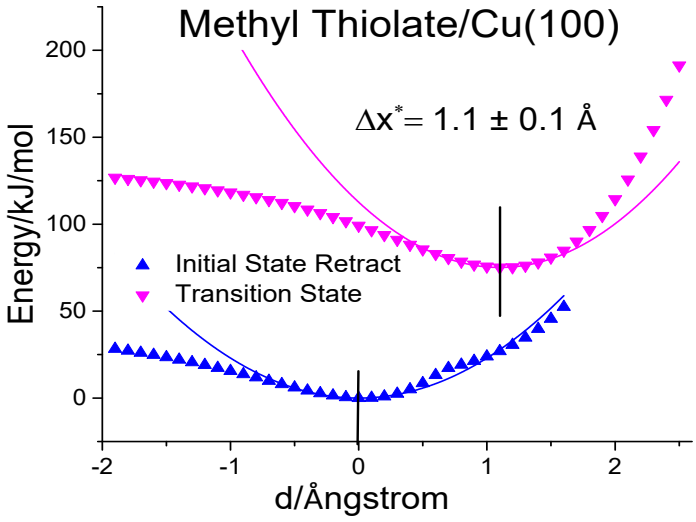

Figure S3: Plot of the calculated energy versus distance for the compression of a methyl thiolate overlayer on copper before background subtraction to remove the long-range interactions.

After calculating the energies of the relaxed, lowest-energy configurations to provide an initial plot of the energies of the initial and transition states as a function of slab separation, a set of single-point calculations are performed to determine the size of the long-range interactions between the slabs as a basis for removing these values from the total energy. These interactions consist of (i) the interaction of the adsorbate with the top slab and (ii) the interaction between the two slabs.

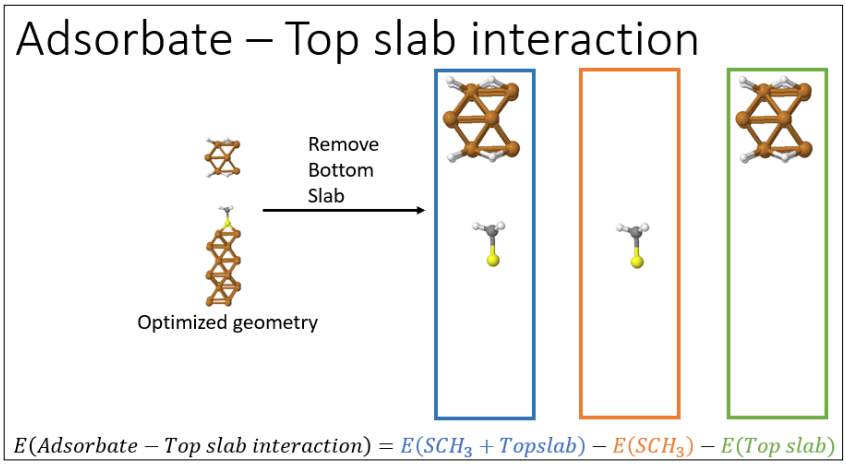

Figure S4: Diagram depicting the procedure for determining the strength of the interaction between the adsorbate and top slab.

(i) *Adsorbate – top slab interactions.* This subtraction is depicted schematically in Figures S5. In the first step, the bottom slab is removed from the relaxed structure to leave only a top slab and the adsorbate. The energy is then calculated for the frozen optimized structures to calculate the energies of:

1) The top slab + adsorbate.
2) The top slab alone (this calculation needs only to be performed once since energy is constant for all structures since these atoms are frozen during relaxation).
3) The adsorbate alone.

The interaction energy is then calculated from:

$$E(adsorbate - top\ slab\ interaction) = E(top\ slab + adsorbate) - E(top\ slab) - E(adsorbate)$$

The results are summarized in Figure S5.

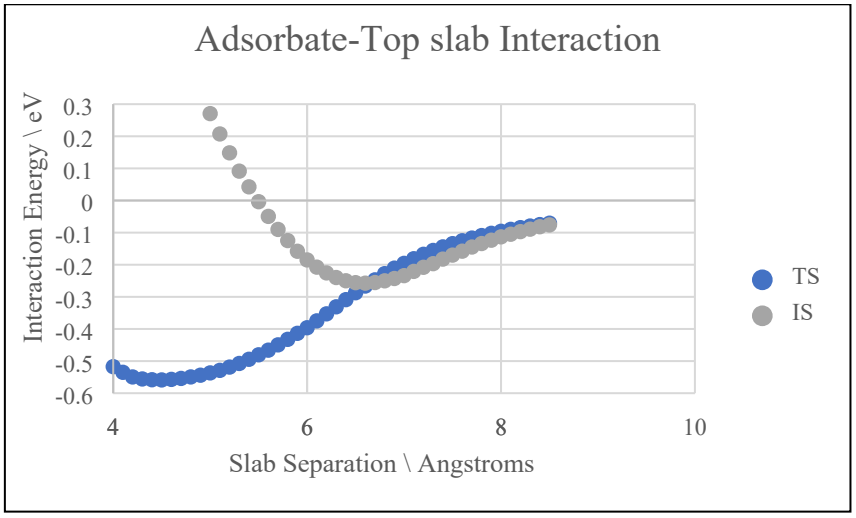

Figure S5: Energies of the adsorbate-top slab interaction as a function of slab separation for the transition (blue) and initial states (grey).

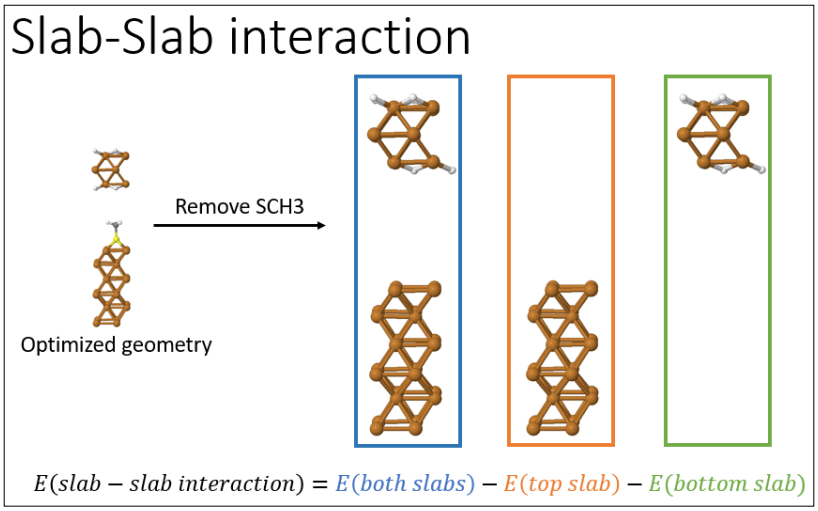

Figure S6: Diagram depicting the procedure for determining the strength of the interaction between the slabs.

(ii) *Slab – slab interactions*: The procedure is illustrated schematically in Figure S7. The adsorbed overlayer is removed from the relaxed structures to provide clean slabs and the following energies are calculated of each structure without allowing the positions of the atoms to relax to calculate the energies of:

1) The top and bottom slab
2) The top slab alone (again, this energy is identical for all calculation)
3) The bottom slab alone

The energy of the interaction is then calculated from:

$$E(slab - slab\ interaction) = E(top\ slab + bottom\ slab) - E(top\ slab) - E(bottom\ slab)$$

The results are summarized in Figure S7.

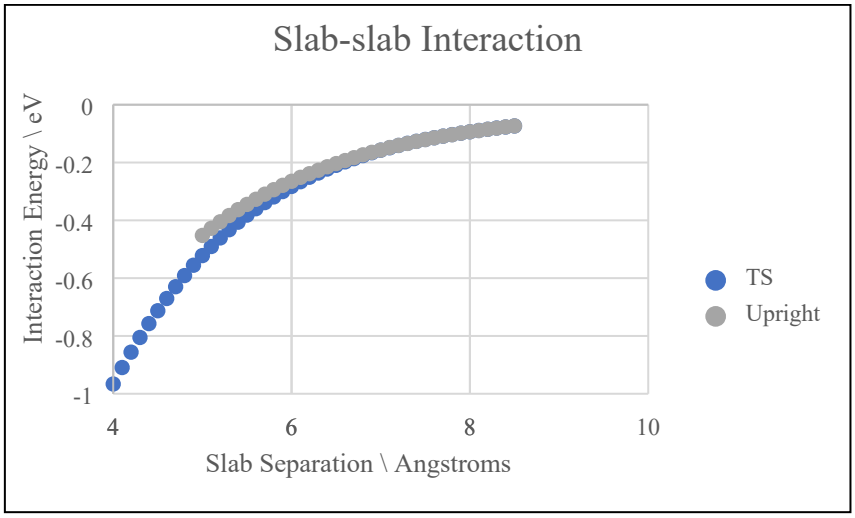

Figure S7: The strength of the slab-slab interaction for the transition state (blue) and initial state (grey).

3. Calibration of Normal Stresses and Reaction Rates. The normal stresses were measured from the ratio of the normal force exerted by the atomic force microscope (AFM) tip divided by the area of the contact. The contact area was obtained from the width of the impression formed by the mechanochemical reaction, which was measured from images collected using the same AFM tip as that used to initiate the reaction, which has an approximately 80 nm diameter, collected at low, non-perturbative loads either from the width of the indent formed on the methyl thiolate overlayer [1] or the width of the wear track formed by sliding.[2] Both sets if data lay on the same curve. Since the resulting image is a convolution of the tip profile with the profile of the indent, the measured widths were divided by a factor of $\sqrt{2}$ to take account of the tip size on the image. The results were summarized in a single plot of contact width versus force on the AFM tip,[2] and the results were in reasonable agreement with a JRK contact model.[3] However, the experimental values were fit to an allosteric function to provide a simple analytical formula for the contact width that was used to calculate the contact area. The normal force was measured from the voltage applied to the piezo tubes in the RHK AFM and converted to a distance using a sensitivity factor of 2.1 ± 0.2 mV/nm measured during the approach of the tip to the surface. This value was assumed to be constant for all experiments. However, the range over which this was calibrated was less than the range of applied voltage and may therefore give deviations from the

true force at high loads.[4] Because the measured cantilever tilt angle in the RHK AFM is ~22.5°, a tilt correction was applied as suggested by Hutter [5] using the values of the length of the cantilever and the length of the tip, obtained from a scanning electron microscope image. These values were used to calculate the normal stress at the center of the contact, which is where the reaction rate was measured. The reaction rate was measured from the depth at the center of the indent as described previously, [1] where the indent ceases to grow at a depth that corresponds to the approximate thickness of the methyl thiolate overlayer (Figure S8).

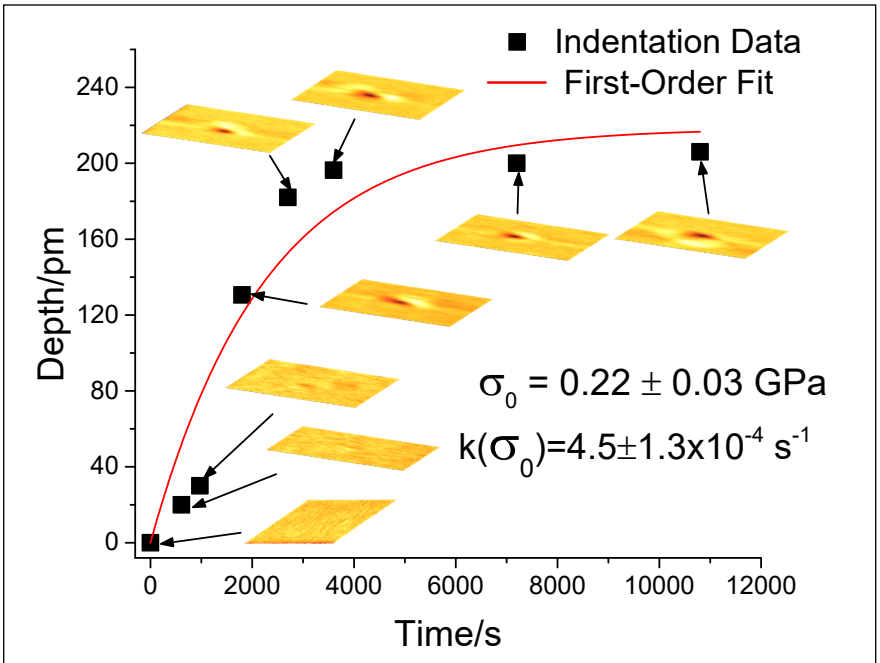

Figure S8: Plot of the indentation depth as a function of contact time for the compression of a methyl thiolate overlayer on Cu(100) for a normal contact stress of 0.22 GPa. The images of the indents are shown in the figure. A fit to the data gives a first-order rate constant of 4.5×10^{-4} s^{-1}.

References

1. A. Boscoboinik, D. Olson, H. Adams, N. Hopper and W. T. Tysoe, *Chemical Communications*, 2020, **56**, 7730-7733.
2. R. Rana, N. Hopper, F. Sidoroff and W. T. Tysoe, *Chemical Science*, 2022, **13**, 12651-12658.
3. K. L. Johnson, Contact mechanics, Cambridge University Press, 1985.
4. E. Thormann, T. Pettersson and P. M. Claesson, *Review of Scientific Instruments*, 2009, **80**, 093701.
5. J. L. Hutter, *Langmuir*, 2005, **21**, 2630-2632.